Quantum Dynamics with Stochastic Non-Hermitian Hamiltonians

Pablo Martinez-Azcona,[1] Aritra Kundu,[1] Avadh Saxena,[2] Adolfo del Campo,[1,3] and Aurélia Chenu[1]
[1]*Department of Physics and Materials Science, University of Luxembourg, L-1511 Luxembourg*
[2]*Theoretical Division, Los Alamos National Laboratory, Los Alamos, New Mexico 87545, USA*
[3]*Donostia International Physics Center, E-20018 San Sebastián, Spain*

(Received 13 August 2024; revised 27 November 2024; accepted 14 May 2025; published 2 July 2025)

We study the quantum dynamics generated by a non-Hermitian Hamiltonian subject to stochastic perturbations in its anti-Hermitian part, describing fluctuating gains and losses. The dynamics averaged over the noise is described by an "antidephasing" master equation. We characterize the resulting state evolution and analyze its purity. The properties of such dynamics are illustrated in a stochastic dissipative qubit. Our analytical results show that adding noise allows for a rich control of the dynamics, stabilizing the lossy state and making state purification possible to a greater variety of steady states.

DOI: 10.1103/5ksl-tjjm

Introduction—Quantum systems are always in contact with an environment. For this reason, any realistic description of quantum dynamics should include the effects of such coupling. The theory of open quantum systems (OQS) offers a wide range of approaches to this end [1,2]. Two prominent approaches involve non-Hermitian (NH) [3–5] and stochastic [6–8] Hamiltonians. NH Hamiltonians are generally associated with effective descriptions that account only for a subset of the total number of degrees of freedom of a quantum mechanical system. They can be obtained by unraveling the Gorini-Kossakowski-Sudarshan-Lindblad (GKSL) equation [9,10] and postselecting the trajectories with no quantum jumps [3,11], or using projector techniques, as often done in quantum optics, nuclear physics, and molecular quantum chemistry [4,5,12–14]. Recently, non-Hermitian Hamiltonians have regained interest because of the novel physical phenomena and topological phases they display [15–21], and of their relation to the quantum Zeno effect [22–27].

NH Hamiltonians generally exhibit complex energy eigenvalues in which the imaginary part describes the lifetime of a state [14,28]. Time evolution ceases to be trace preserving due to the leakage of probability density between the subspace under consideration and that associated with the remaining degrees of freedom. The evolution is made trace preserving (TP) by renormalizing the density matrix at all times, which renders the evolution nonlinear in the state [29–33]. TP nonlinear dynamics has been realized experimentally by postselection of dissipative evolution, i.e., discarding the trajectories with quantum jumps [34,35]. In this setting, the renormalization of the trace comes naturally as a restriction to the subset of trajectories with no quantum jumps. This allowed the study of a plethora of dissipation-induced phenomena [36–40].

Stochastic Hamiltonians allow for a treatment of OQS in which the effect of the environment is modeled through the noise statistics [6,8,41]. These appear naturally in the stochastic Schrödinger equations obtained by unraveling the GKSL equation in quantum trajectories [29,42,43]. Stochastic Hamiltonians have been used to engineer many-body and long-range interactions [7], and their behavior beyond the noise average relates to quantum information scrambling [44].

While the stability of certain features of NH Hamiltonians under noise has recently been investigated [45], non-Hermitian Hamiltonians are typically studied in a deterministic setting. In this Letter, we go beyond this paradigm by studying the dynamics of NH Hamiltonians subject to classical noise. This is particularly relevant since current experimental realizations of NH dynamics use noisy intermediate scale quantum (NISQ) devices [46]. We choose to focus on the effect of fluctuations on the anti-Hermitian part, which arise from noise in experimental setups [34] or in homodyne detection of the degenerate parametric oscillator [47]; the possible experimental setups are detailed in [48]. By considering the stochastic dynamics of a fluctuating non-Hermitian system, we unveil a new kind of averaged master equation, that we call "antidephasing" because of the structure of the dissipator—which involves anticommutators instead of the commutators commonly encountered in the GKSL dephasing master equation. We derive an exact evolution equation for the purity and characterize its dynamics. Specifically, we identify the stable steady states in terms of the eigenvalues and eigenstates of the Liouvillian. We illustrate the anti-dephasing dynamics in an experimentally feasible stochastic dissipative qubit [34,48,58], in which case we find a novel noise-induced phase, where the noise stabilizes the originally lossy state.

Dynamics under anti-Hermitian fluctuations—We consider a system with Hermitian Hamiltonian $\hat{H}_0$ that is subject to classical noise coupled to the anti-Hermitian operator $i\hat{L}$, i.e.,

$$\hat{H}_t = \hat{H}_0 - i(1 + \sqrt{2\gamma}\xi_t)\hat{L}. \quad (1)$$

This describes fluctuations around the mean in the Hermitian operator $\hat{L} = \hat{L}^\dagger$, positive $\hat{L} \geq 0$ operators, with standard deviation $\sqrt{2\gamma}$, and could be amenable to experimental implementation [48]. The classical noise is taken as Gaussian real white noise for simplicity, characterized by $\mathbb{E}(\xi_t) = 0$ and $\mathbb{E}(\xi_t \xi_{t'}) = \delta(t - t')$, where $\mathbb{E}(\bullet)$ denotes the classical stochastic average. The (unnormalized) system density matrix for a single trajectory $\tilde{\varrho}_t$ evolves, over a small time increment, as $\tilde{\varrho}_{t+\mathrm{d}t} = \hat{U}_{\mathrm{d}t}\tilde{\varrho}_t\hat{U}_{\mathrm{d}t}^\dagger$, where the propagator $\hat{U}_{\mathrm{d}t} = \exp(-i\hat{H}_0\mathrm{d}t - \hat{L}\mathrm{d}t - \sqrt{2\gamma}\hat{L}\mathrm{d}W_t)$ depends on the Wiener process $\mathrm{d}W_t = \xi_t\mathrm{d}t$. For Gaussian white noise, the latter obeys Itō's rules [59]: $\mathrm{d}W_t^2 = \mathrm{d}t$ and $(\mathrm{d}W_t)^n = 0,\ \forall\ n > 2$. Expanding the exponential dictating the evolution of the density matrix with these rules, we find a stochastic differential equation (SDE) for its evolution,

$$\mathrm{d}\tilde{\varrho}_t = \left(-i[\hat{H}_0, \tilde{\varrho}_t] - \{\hat{L}, \tilde{\varrho}_t\} + \gamma\{\hat{L}, \{\hat{L}, \tilde{\varrho}_t\}\}\right)\mathrm{d}t - \sqrt{2\gamma}\{\hat{L}, \tilde{\varrho}_t\}\mathrm{d}W_t. \quad (2)$$

We denote $\tilde{\rho} \equiv \mathbb{E}(\tilde{\varrho})$ the noise-averaged density matrix and use the tilde $\tilde{\bullet}$ to highlight that it is not normalized. Trace preservation can be imposed either by (i) renormalizing all single trajectories and then averaging over the noise [26,29,43,60], or (ii) first averaging over the noise, and only then imposing trace preservation. These two approaches will generally yield different dynamics. We focus on the latter to capture the evolution of ensembles of trajectories analytically and defer the former for future analysis.

The average over the noise of the unnormalized evolution reads

$$\frac{\mathrm{d}\tilde{\rho}_t}{\mathrm{d}t} = -i[\hat{H}_0, \tilde{\rho}_t] - \{\hat{L}, \tilde{\rho}_t\} + \gamma\{\hat{L}, \{\hat{L}, \tilde{\rho}_t\}\} \equiv \tilde{\mathcal{L}}[\tilde{\rho}_t], \quad (3)$$

for the noise-averaged density matrix, where $\tilde{\mathcal{L}}[\bullet]$ denotes the Liouvillian superoperator, which is not necessarily trace preserving. This master equation can be formally solved as $\tilde{\rho}_t = e^{\tilde{\mathcal{L}}t}[\hat{\rho}_0]$. Imposing trace preservation at the average level yields the nonlinear master equation

$$\begin{aligned}\frac{\mathrm{d}\hat{\rho}_t}{\mathrm{d}t} &= \tilde{\mathcal{L}}[\hat{\rho}_t] - \mathrm{Tr}(\tilde{\mathcal{L}}[\hat{\rho}_t])\hat{\rho}_t \\ &= -i[\hat{H}_0, \hat{\rho}_t] - \{\hat{L}, \hat{\rho}_t\} + \gamma\{\hat{L}, \{\hat{L}, \hat{\rho}_t\}\} \\ &\quad + 2\mathrm{Tr}(\hat{L}\hat{\rho}_t)\hat{\rho}_t - 4\gamma\mathrm{Tr}(\hat{L}^2\hat{\rho}_t)\hat{\rho}_t, \end{aligned} \quad (4)$$

the solution of which is given by normalizing the nontrace-preserving (nTP) evolution, i.e., $\hat{\rho}_t \equiv \tilde{\rho}_t/\mathrm{Tr}(\tilde{\rho}_t) = e^{\tilde{\mathcal{L}}t}[\hat{\rho}_0]/\mathrm{Tr}(e^{\tilde{\mathcal{L}}t}[\hat{\rho}_0])$. Since the NH Hamiltonian is stochastic, the evolution leads to quantum jumps—terms of the form $\gamma\hat{L}\hat{\rho}_t\hat{L}$. Note that this master equation is not of GKSL form; instead, the jump operators act on the density matrix through a double anticommutator and do not conserve the norm of the state. We term this new dissipator "antidephasing." A more standard form is detailed in [48]. Similar equations, with a double anticommutator but with a minus sign, appear when studying the adjoint Liouvillian with fermionic jumps and evolving operators [61,62].

Note that, in general, the unnormalized evolution (3) can be trace decreasing (TD), trace preserving (TP), or trace increasing (TI). While TD dynamics can easily be interpreted through postselection, e.g., with *hybrid Liouvillians* [63–65], TI evolutions are conceptually challenging; even if sometimes deemed nonphysical [66] they can describe a biased ensemble of trajectories [67–72]. Remarkably, the present TI dynamics can always be made TD or TP by a gauge transformation in the master equation, namely, using an imaginary offset $-ia$ in (1), as we detail in [48]. This is because such a transformation rigidly shifts the Liouvillian spectrum, conserving the relative differences between eigenvalues and, hence, the dynamical features.

We now characterize the dynamics generated by (4) in terms of the purity evolution and the stable steady states in the general setup before illustrating them in a stochastic dissipative qubit.

Purity dynamics—The purity $P_t = \mathrm{Tr}(\hat{\rho}_t^2)$ quantifies how mixed a state is, even when its trace evolves in time. For antidephasing dynamics, it evolves according to the differential equation

$$\begin{aligned}\partial_t P_t &= -4\mathrm{Tr}(\hat{L}\hat{\rho}_t^2) + 4\gamma\left(\mathrm{Tr}(\hat{L}^2\hat{\rho}_t^2) + \mathrm{Tr}(\hat{L}\hat{\rho}_t\hat{L}\hat{\rho}_t)\right) \\ &\quad + 4\mathrm{Tr}(\hat{L}\hat{\rho}_t)P_t - 8\gamma\mathrm{Tr}(\hat{L}^2\hat{\rho}_t)P_t. \end{aligned} \quad (5)$$

Evaluating this expression at $t = 0$ yields the decoherence time $1/\tau_P \equiv \partial_t P_t|_{t=0}$. Whenever the state is pure, $\hat{\rho}_t = |\Psi_t\rangle\langle\Psi_t|$, the terms coming from the deterministic anti-Hermitian part cancel out and the purity evolution $\partial_t P_t = -4\gamma\mathrm{Var}_\Psi(\hat{L})$ is dictated by the variance $\mathrm{Var}_\Psi(\hat{L}) = \langle\Psi_t|\hat{L}^2|\Psi_t\rangle - \langle\Psi_t|\hat{L}|\Psi_t\rangle^2$. Thus, initial pure states exhibit a purity decay unless they are eigenstates of $\hat{L}$, in this case, the purity remains constant at first order in t ($\tau_P \to \infty$). This result is identical to the decoherence time of pure states in a dephasing channel and quantum Brownian motion [1,73,74]. Interestingly, this expression contains out-of-time-order terms reminiscent of OTOC's [44] and generalizes the known evolution for NH Hamiltonians [30].

Long time dynamics: Stable steady states—To characterize the long-time dynamics, we use the right and left eigendecompositions of the Liouvillian superoperator, $\tilde{\mathcal{L}}[\tilde{\rho}_\nu] = \lambda_\nu\tilde{\rho}_\nu$ and $\tilde{\mathcal{L}}^\dagger[\tilde{\rho}_\nu^{(\mathrm{L})}] = \lambda_\nu^*\tilde{\rho}_\nu^{(\mathrm{L})}$, respectively. We define the eigenoperator basis as $\hat{\sigma}_\nu = \tilde{\rho}_\nu/\mathrm{Tr}(\tilde{\rho}_\nu)$ if the operator has nonzero trace and as $\hat{\sigma}_\nu = \tilde{\rho}_\nu$ if the operator is traceless. Furthermore, the eigenstate is *physical* when it has unit trace, $\mathrm{Tr}(\hat{\sigma}_\nu) = 1$, and is positive semidefinite $\hat{\sigma}_\nu \geq 0$. The basis is ordered such that the physical states appear first $0 \leq \nu < N_{\mathrm{p}}$, the traceful states appear second $N_{\mathrm{p}} \leq \nu < N_{\mathrm{T}}$, and the traceless states come last. In each subset, the states are further ordered by decreasing $\mathrm{Re}(\lambda_\nu)$. Assuming the Liouvillian $\tilde{\mathcal{L}}$ to be diagonalizable, the evolution of the density matrix in this operator basis follows as

$$\hat{\rho}_t = \frac{\sum_{\nu=0}^{N^2-1} c_\nu e^{\lambda_\nu t} \hat{\sigma}_\nu}{\sum_{\mu=0}^{N_{\mathrm{T}}-1} c_\mu e^{\lambda_\mu t}} \overset{t\to\infty}{\sim} \hat{\sigma}_0 + e^{-\Delta t} \sum_{\nu \in \mathbb{M}_2} \frac{c_\nu e^{i\omega_\nu t}}{c_0} \hat{\sigma}_\nu, \quad (6)$$

where the coefficients are $c_\nu = \mathrm{Tr}(\hat{\sigma}_\nu^{(\mathrm{L})} \hat{\rho}_0)/\mathrm{Tr}(\hat{\sigma}_\nu^{(\mathrm{L})} \hat{\sigma}_\nu)$. All the physical states ($\hat{\sigma}_\nu$ with $\nu < N_{\mathrm{p}}$) are steady states. However, only those whose eigenvalues have the largest real part $\hat{\sigma}_0$ are stable under all perturbations [75].

At long times, the stable steady state $\hat{\sigma}_0$ is the eigenoperator associated with the eigenvalue with the largest real part over which there is initial support, i.e., $\mathrm{Re}(\lambda_0) = \max_\nu \mathrm{Re}(\lambda_\nu)$ such that $c_\nu \neq 0$. The corrections to this state are suppressed at a rate dictated by the "dissipative gap" $\Delta = \mathrm{Re}(\lambda_0 - \lambda_1)$. They can oscillate with a frequency $\omega_\nu = \mathrm{Im}(\lambda_\nu)$, depending on the presence or absence of complex eigenvalues in the set of states with the second largest real part, denoted by $\mathbb{M}_2$.

The long-time limit above (6) assumes that the largest eigenvalue is real and nondegenerate. In a more general case, denoting by $\mathbb{M}_1$ the set of states with the largest real part among those on which the initial state has nonzero support, the steady state follows as $\hat{\rho}^{\mathrm{S}} = [(\sum_{\nu \in \mathbb{M}_1}^{N^2-1} c_\nu e^{i\omega_\nu t} \hat{\sigma}_\nu)/(\sum_{\mu \in \mathbb{M}_1}^{N_{\mathrm{T}}-1} c_\mu e^{i\omega_\mu t})]$.

Illustration: The stochastic dissipative qubit—Many of the exciting phenomena displayed by non-Hermitian Hamiltonians have been experimentally observed in a dissipative qubit [34–40]. The setting corresponds to the Lindblad evolution of a three-level system $\{|g\rangle, |e\rangle, |f\rangle\}$, where all quantum jumps from $|e\rangle$ to $|g\rangle$ are discarded. This postselection process leads to the non-Hermitian Hamiltonian $\hat{H} = J\hat{\sigma}_x - i\Gamma\hat{\Pi}$, where J is the hopping between $|e\rangle$ and $|f\rangle$, $\Gamma \geq 0$ is the decay rate from $|e\rangle$ to $|g\rangle$, and $\hat{\Pi} = |e\rangle\langle e|$ denotes the projector over state $|e\rangle$. The (shifted) spectrum $\varepsilon_\pm + i(\Gamma/2) = \pm\sqrt{J^2 - \Gamma^2/4}$ is real for $J \geq \Gamma/2$ and imaginary for $J < \Gamma/2$. These two regimes respectively correspond to (passive) $\mathcal{PT}$ unbroken and broken symmetry phases [76].

In this Letter, we are interested in the effect of noise in the anti-Hermitian part of the Hamiltonian. We thus consider a stochastic dissipative qubit (SDQ) with time-dependent Hamiltonian

$$\hat{H}_t^{\mathrm{SDQ}} = J\hat{\sigma}_x - i\Gamma(1 + \sqrt{2\gamma}\xi_t)\hat{\Pi}, \quad (7)$$

which physically corresponds to considering Gaussian fluctuations in the decay parameter Γ, with strength γ. This system can be experimentally realized with superconducting qubits [34], where noise is known to be present in the setup [48], or in trapped ions [58], where noise may be easier to tune [48]. The master equation (4) for this system reads

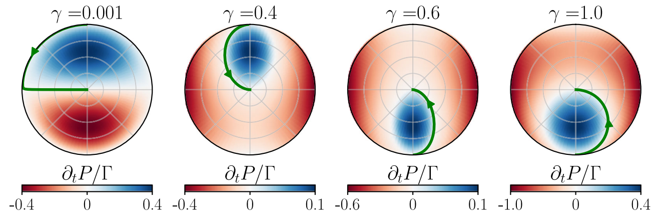

FIG. 1. Purity evolution for different strengths of the noise, where we set $\Gamma = 1$, as given by (9) in a cross section of the Bloch sphere. The stable steady states correspond to parameters $(\Gamma/J, \gamma J)$, the hopping being increased in the range $J \in [10^{-2}, 10^2]$ (green line). See Ref. [48] for the analytical expressions.

$$\partial_t \hat{\rho}_t = -iJ[\hat{\sigma}_x, \hat{\rho}_t] - (\Gamma - \gamma\Gamma^2)\{\hat{\Pi}, \hat{\rho}_t\} + 2\gamma\Gamma^2 \hat{\Pi}\hat{\rho}_t\hat{\Pi} + (2\Gamma - 4\gamma\Gamma^2)\mathrm{Tr}(\hat{\Pi}\hat{\rho}_t)\hat{\rho}_t. \quad (8)$$

The trace of the Liouvillian acting on any state reads $\mathrm{Tr}(\tilde{\mathcal{L}}[\hat{\rho}]) = (4\gamma\Gamma^2 - 2\Gamma)\mathrm{Tr}(\hat{\Pi}\hat{\rho})$. Note that it depends on the population of the $|e\rangle$ state, since $\mathrm{Tr}(\hat{\Pi}\hat{\rho}) = \rho_{ee}$. Therefore the dynamics inhibits the state $|e\rangle$ when $4\gamma\Gamma^2 - 2\Gamma < 0$ and favors it when $4\gamma\Gamma^2 - 2\Gamma > 0$. Thus, the dynamics exhibits a transition at $\gamma^* = 1/(2\Gamma)$. At this critical value, the trace of the Liouvillian vanishes, the dynamics is completely positive and trace preserving (CPTP), and its generator admits the standard GKSL form, with jump operator $\hat{\Pi}$ and rate Γ. The dynamics is trivially unitary when the Hamiltonian is Hermitian ($\Gamma = 0$). The noise can be used to tune the success rate, i.e., the number of trajectories with no jumps. Assuming that the trace of the unnormalized state gives the success rate, it reads $\mathrm{Tr}(\tilde{\rho}_t) = e^{-2\Gamma(1-2\gamma\Gamma)t}(c_0 + JB\int_0^t e^{-JB\tau}\rho_{ff}(\tau)\mathrm{d}\tau)$ where $JB = 2\Gamma(2\gamma\Gamma - 1)$. If the noise increases, the overall decay will be slower; thus, a stronger noise γ could be used to mitigate the decay of the success rate, especially near the critical value γ^*.

Every state of a qubit can be expressed in the Bloch sphere as $\hat{\rho}_t = \frac{1}{2}(\hat{\mathbb{1}} + \mathbf{r}_t \cdot \hat{\boldsymbol{\sigma}})$, where $\hat{\boldsymbol{\sigma}}$ is a vector containing the Pauli matrices [66]. Expressing the Bloch vector $\mathbf{r}_t = (x_t, y_t, z_t)$ in spherical coordinates (r_t, θ_t, ϕ_t), the purity (5) evolves for any state $\hat{\rho}_t$ as

$$\partial_t P_t = \Gamma r_t[(2\gamma\Gamma - 1)(r_t^2 - 1)\cos\theta_t - \gamma\Gamma r_t \sin^2\theta_t]. \quad (9)$$

Note that this expression shows a change in behavior at the TD-TI transition $\Gamma\gamma = \frac{1}{2}$. When $\Gamma\gamma < \frac{1}{2}$, the purifying states are in the north hemisphere of the Bloch sphere, while for $\Gamma\gamma > \frac{1}{2}$, these states are shifted to the southern hemisphere, see Fig. 1. More details on the steady states are provided in [48].

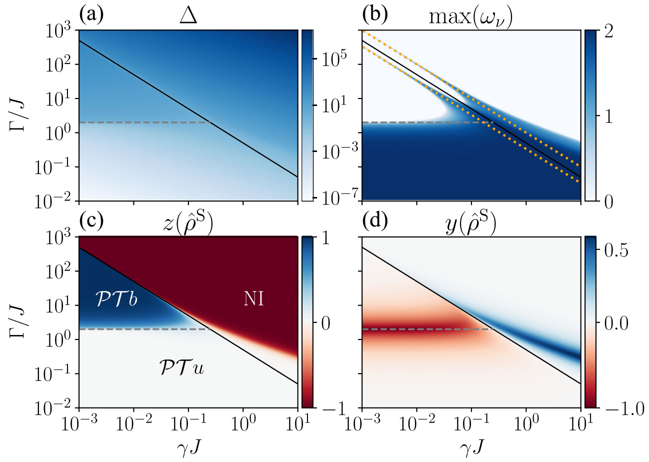

FIG. 2. Spectral and steady-state phase diagrams: (a) Dissipative gap Δ dictating the timescale of convergence to the steady state, (b) maximum imaginary part of the eigenvalues ω_ν, (c) z, and (d) y components of the Bloch vector for the stable steady state $\hat{\rho}^{\mathrm{S}}$. The z coordinate (c) characterizes the three different phases to which the dynamics can stabilize. The dimensionless parameters determine the noise strength γJ and the decay rate Γ/J. The transition to the noise-induced phase is at $\gamma^* = 1/(2\Gamma)$ (black line). The transition from $\mathcal{PT}$ broken to the $\mathcal{PT}$ unbroken phase happens at $\Gamma/J = 2$ (gray dashed line). In (b) the power laws $\gamma = 1/(3\Gamma)$ and $\gamma = 1/\Gamma$ are also shown (orange dotted lines).

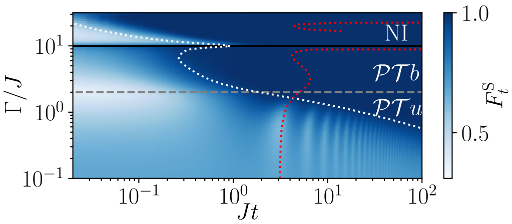

FIG. 3. Fidelity between the time-evolved state and the stable steady state as a function of the decay parameter Γ and time for noise strength $\gamma J = 0.05$. $\mathcal{PT}$u to $\mathcal{PT}$b phase transition (gray dashed) and $\mathcal{PT}$b to NI phase transition (black). Timescales of the dissipative gap Δ^{-1} (white dotted) and oscillatory dynamics $2\pi/\omega$ (red dotted).

We now investigate the spectral properties of the SDQ Liouvillian (8). The phase diagrams in Fig. 2 have three distinct phases: at weak noise γ, the notions of $\mathcal{PT}$ broken $\Gamma/J > 2$ and unbroken $\Gamma/J < 2$ symmetry of the NH Hamiltonian govern the dynamics, while at large noise strength, we see a transition to the TI dynamics at γ^*. We refer to these phases as $\mathcal{PT}$ broken ($\mathcal{PT}$b), $\mathcal{PT}$ unbroken ($\mathcal{PT}$u), and noise induced (NI). Figure 2(a) shows the dissipative gap Δ as a function of the noise strength γ and the decay rate Γ. In the $\mathcal{PT}$u phase, the dissipative gap is very small; thus, the convergence to the stable steady state is very slow. Interestingly, a small *residual damping rate* was observed experimentally in this phase [34,48]. In the $\mathcal{PT}$b phase, the gap is larger. Therefore, the steady state is reached faster than in the $\mathcal{PT}$u phase. In the NI phase, the gap is very large, ensuring fast convergence to the stable steady state [cf. Eq. (6)]. Note that the gap is always smaller around the transition to the NI phase, which implies that the GKSL dynamics has slower convergence to the stable steady state. Figure 2(b) shows the maximum imaginary part of the eigenvalues of the Lindbladian, which dictate the oscillatory behavior of the dynamics. Deep in the $\mathcal{PT}$b and NI phases, the imaginary part vanishes, implying that the dynamics is not oscillatory. However, it is nonzero in the $\mathcal{PT}$u phase. This fact, along with the very small dissipative gap, shows what features of the $\mathcal{PT}$u phase survive the application of classical noise.

We now characterize the nondegenerate stable steady state $\hat{\rho}^{\mathrm{S}}$. Figure 2(c) shows the z component of the Bloch vector of $\hat{\rho}^{\mathrm{S}}$, which reads $z(\hat{\rho}^{\mathrm{S}}) = -\lambda_0(\lambda_0 - AJ)/[4J^2 + \lambda_0(\lambda_0 - AJ)]$ [48], where λ_0 denotes the eigenvalue with the largest real part and $A = (\Gamma/J)(\gamma\Gamma - 1)$ is a constant. In the $\mathcal{PT}$u phase, the z component is close to zero, and the steady state is close to the maximally mixed state. Thus, when a very small noise is added to the $\mathcal{PT}$ symmetric NH Hamiltonian, the time evolution leads to a highly mixed state at very long times. In the $\mathcal{PT}$b phase, z is close to unity—so the stable steady state is close to $|f\rangle$, as losses induced by Γ remove all population in the $|e\rangle$ state. In the NI phase, the steady state is $|e\rangle$—the state that originally leaked to the ground state. This can be interpreted as a noise-induced transition to stability [77] of the originally unstable state, a feature shared by other noisy dynamics [44]. The y Bloch coordinate phase diagram in Fig. 2(d) shows that the transition from the mixed state to the $|f\rangle$ ($|e\rangle$) state happens by acquiring a negative (positive) value of the y coordinate in the Bloch sphere. The analytic expression for this quantity is $y(\hat{\rho}^{\mathrm{S}}) = 2\lambda_0 J/[4J^2 + \lambda_0(\lambda_0 - AJ)]$ [48].

Let us now turn to the dynamics generated by the master equation (8). The dynamics can be solved numerically in two complementary ways [48]. We characterize the distinguishability between the evolving and stable steady states using the Uhlmann fidelity $F_t^{\mathrm{S}} = F(\hat{\rho}_t, \hat{\rho}^{\mathrm{S}})$ [78,79], which admits a compact form in a qubit system [48,80,81]. Figure 3 shows the evolution of the fidelity as a function of time and the decay parameter Γ for a small noise, $\gamma J = 0.05$. This value ensures that the three different phases are manifested: (i) For $\Gamma/J < 2$, the system is in the $\mathcal{PT}$u phase, and the fidelity to the steady state exhibits the anticipated oscillatory behavior until it vanishes at a time close to the inverse dissipative gap $t \sim \Delta^{-1}$ (white dotted line). The period of these oscillations is perfectly characterized by $2\pi/\omega$ where $\omega = \max_\nu \mathrm{Im}(\lambda_\nu)$, as highlighted by the red dotted line. Note that this oscillatory frequency is affected by the increase of Γ as we approach the $\mathcal{PT}$ phase transition, as also observed experimentally in the dissipative qubit [34]. (ii) For $2 < \Gamma/J < 1/(2J\gamma)$, the system is in the $\mathcal{PT}$b phase, with a larger dissipative gap [cf. Fig. 2(a)], and thus a faster convergence to the steady state. Interestingly, the oscillatory timescale can be finite outside the $\mathcal{PT}$u phase as ω does not vanish identically. In particular, it shows minima at $\Gamma = 1/(3\gamma)$ and $\Gamma = 1/\gamma$, as observed in Fig. 2(b). Exactly at the transition $\Gamma = 1/(2\gamma)$, the dynamics is CPTP, and its convergence is slower, as explained by the smaller gap at the transition line. (iii) For $\Gamma/J > 1/(2J\gamma)$, the system is in the NI phase and exhibits the fastest convergence to the steady state. Experimentally, the decay rate is $\Gamma = 6.7\ \mu s^{-1}$ [34], which upper bounds the noise strength $\gamma < \gamma^* \approx 0.074\ \mu s$ given that no NI phase was observed.

Conclusions—We have considered the time evolution governed by a fluctuating non-Hermitian Hamiltonian describing a quantum mechanical system subject to stochastic gain and loss. The resulting noise-averaged dynamics is described by a novel antidephasing master equation beyond the GKSL form. We characterized the purity dynamics and found that the stable steady states live in the Liouvillian eigenspace whose eigenvalues have the largest real part. The salient features of such dynamics are manifested in a stochastic dissipative qubit. The addition of noise allows for control over the steady states and the convergence rate. We find three main dynamical phases: the $\mathcal{PT}$ unbroken and broken regimes, complemented with a noise-induced phase. Our results are amenable to current experimental platforms realizing non-Hermitian evolution and provide a framework to capture the effect of noise, as exemplified by the residual damping rate [34]. Our findings suggest that engineering fluctuating operators associated with gain and loss may open new avenues for quantum state preparation [82]. Our results may also be applied to understand the stability of imaginary time evolution [83] against classical noise.

Acknowledgments—We thank Oskar Prosniak, Kohei Kawabata, Martin Plenio, Raphaël Chétrite, and Yogesh Joglekar for their insightful discussions and Juan P. Garrahan and Shiue-Yuan Shiau for comments on the manuscript. This research was funded by the Luxembourg National Research Fund (FNR, Attract grant QOMPET 15382998 and Grants No. 17132054 and No. 17233877). The work at Los Alamos was supported by the U.S. Department of Energy.

[1] H.-P. Breuer and F. Petruccione, *The Theory of Open Quantum Systems* (Oxford University Press, Oxford, 2007).
[2] A. Rivas and S. F. Huelga, *Open Quantum Systems* (Springer, Berlin, Heidelberg, 2012).
[3] Y. Ashida, Z. Gong, and M. Ueda, Adv. Phys. **69**, 249 (2020).
[4] M. B. Plenio and P. L. Knight, Rev. Mod. Phys. **70**, 101 (1998).
[5] N. Moiseyev, *Non-Hermitian Quantum Mechanics* (Cambridge University Press, Cambridge, England, 2011).
[6] A. A. Budini, Phys. Rev. A **64**, 052110 (2001).
[7] A. Chenu, M. Beau, J. Cao, and A. del Campo, Phys. Rev. Lett. **118**, 140403 (2017).
[8] A. Kiely, Europhys. Lett. **134**, 10001 (2021).
[9] V. Gorini, A. Kossakowski, and E. C. G. Sudarshan, J. Math. Phys. (N.Y.) **17**, 821 (1976).
[10] G. Lindblad, Commun. Math. Phys. **48**, 119 (1976).
[11] F. Roccati, G. M. Palma, F. Ciccarello, and F. Bagarello, Open Syst. Inf. Dyn. **29**, 2250004 (2022).
[12] H. Feshbach, Ann. Phys. (N.Y.) **5**, 357 (1958).
[13] H. Feshbach, Ann. Phys. (N.Y.) **19**, 287 (1962).
[14] C. Cohen-Tannoudji, J. Dupont-Roc, and G. Grynberg, *Atom—Photon Interactions: Basic Process and Appilcations* (Wiley, New York, 1998).
[15] H. Shen, B. Zhen, and L. Fu, Phys. Rev. Lett. **120**, 146402 (2018).
[16] Z. Gong, Y. Ashida, K. Kawabata, K. Takasan, S. Higashikawa, and M. Ueda, Phys. Rev. X **8**, 031079 (2018).
[17] K. Kawabata, Y. Ashida, H. Katsura, and M. Ueda, Phys. Rev. B **98**, 085116 (2018).
[18] S. Yao and Z. Wang, Phys. Rev. Lett. **121**, 086803 (2018).
[19] K. Takata and M. Notomi, Phys. Rev. Lett. **121**, 213902 (2018).
[20] H. Yang, C. Wang, T. Yu, Y. Cao, and P. Yan, Phys. Rev. Lett. **121**, 197201 (2018).
[21] T. Guo, K. Kawabata, R. Nakai, and S. Ryu, Phys. Rev. B **108**, 075108 (2023).
[22] G. Allcock, Ann. Phys. (N.Y.) **53**, 253 (1969).
[23] L. S. Schulman, Phys. Rev. A **57**, 1509 (1998).
[24] E. W. Streed, J. Mun, M. Boyd, G. K. Campbell, P. Medley, W. Ketterle, and D. E. Pritchard, Phys. Rev. Lett. **97**, 260402 (2006).
[25] J. Echanobe, A. del Campo, and J. G. Muga, Phys. Rev. A **77**, 032112 (2008).
[26] V. Dubey, R. Chetrite, and A. Dhar, J. Phys. A **56**, 154001 (2023).
[27] K. Snizhko, P. Kumar, and A. Romito, Phys. Rev. Res. **2**, 033512 (2020).
[28] G. Gamow, Z. Phys. **51**, 204 (1928).
[29] H. J. Carmichael, *Statistical Methods in Quantum Optics 2* (Springer, Berlin, 2008).
[30] D. C. Brody and E.-M. Graefe, Phys. Rev. Lett. **109**, 230405 (2012).
[31] S. Alipour, A. Chenu, A. T. Rezakhani, and A. del Campo, Quantum **4**, 336 (2020).
[32] M. R. Geller, Adv. Quantum Technol. **6**, 2200156 (2023).
[33] J. Rembieliński and P. Caban, Quantum **5**, 420 (2021).
[34] M. Naghiloo, M. Abbasi, Y. N. Joglekar, and K. W. Murch, Nat. Phys. **15**, 1232 (2019).
[35] W. Chen, M. Abbasi, Y. N. Joglekar, and K. W. Murch, Phys. Rev. Lett. **127**, 140504 (2021).
[36] M. Abbasi, W. Chen, M. Naghiloo, Y. N. Joglekar, and K. W. Murch, Phys. Rev. Lett. **128**, 160401 (2022).
[37] S. Erdamar, M. Abbasi, B. Ha, W. Chen, J. Muldoon, Y. Joglekar, and K. W. Murch, Phys. Rev. Res. **6**, L022013 (2024).
[38] P. M. Harrington, E. J. Mueller, and K. W. Murch, Nat. Rev. Phys. **4**, 660 (2022).
[39] W. Chen, M. Abbasi, B. Ha, S. Erdamar, Y. N. Joglekar, and K. W. Murch, Phys. Rev. Lett. **128**, 110402 (2022).

[40] Y. Wang, K. Snizhko, A. Romito, Y. Gefen, and K. Murch, Phys. Rev. A **108**, 013712 (2023).
[41] N. Van Kampen, *Stochastic Processes in Physics and Chemistry*, North-Holland Personal Library (Elsevier Science, New York, 2011).
[42] H. M. Wiseman, Quantum Semiclass. Opt. **8**, 205 (1996).
[43] H. M. Wiseman and G. J. Milburn, *Quantum Measurement and Control* (Cambridge University Press, Cambridge, England, 2009).
[44] P. Martinez-Azcona, A. Kundu, A. del Campo, and A. Chenu, Phys. Rev. Lett. **131**, 160202 (2023).
[45] J. Wiersig, Phys. Rev. A **101**, 053846 (2020).
[46] J. Preskill, Quantum **2**, 79 (2018).
[47] H. Carmichael, *An Open Systems Approach to Quantum Optics* (Springer, Berlin, 1991).
[48] See Supplemental Material at http://link.aps.org/supplemental/10.1103/5ksl-tjjm, which includes Refs. [49–57], for study of the gauge transformations of the antidephasing master equation, discussion of possible experimental realizations of stochastic non-Hermitian Hamiltonians, further details on the dynamics and Liouvillian spectra of the SDQ, comparison of the antidephasing Liouvillian to hybrid and tilted Liouvillians, and expression of it in a more standard form.
[49] E. Piñol, T. K. Mavrogordatos, D. Keys, R. Veyron, P. Sierant, M. Angel García-March, S. Grandi, M. W. Mitchell, J. Wehr, and M. Lewenstein, Phys. Rev. Res. **6**, L032057 (2024).
[50] J. A. Sherman, M. J. Curtis, D. J. Szwer, D. T. C. Allcock, G. Imreh, D. M. Lucas, and A. M. Steane, Phys. Rev. Lett. **111**, 180501 (2013).
[51] E. Brion, L. H. Pedersen, and K. Mølmer, J. Phys. A **40**, 1033 (2007).
[52] J. G. Muga, J. Echanobe, A. del Campo, and I. Lizuain, J. Phys. B **41**, 175501 (2008).
[53] J. A. Gyamfi, Eur. J. Phys. **41**, 063002 (2020).
[54] M.-D. Choi, Linear Algebra Appl. **10**, 285 (1975).
[55] A. Jamiołkowski, Rep. Math. Phys. **3**, 275 (1972).
[56] R. Nickalls, Math. Gazette **77**, 354 (1993).
[57] S. H. Strogatz, *Nonlinear Dynamics and Chaos* (CRC Press, Boca Raton, 2018).
[58] A. Quinn, J. Metzner, J. E. Muldoon, I. D. Moore, S. Brudney, S. Das, D. T. C. Allcock, and Y. N. Joglekar, arXiv:2304.12413.
[59] C. W. Gardiner, *Handbook of Stochastic Methods* (springer, Berlin, 1985), Vol. 3.
[60] T. Benoist, C. Bernardin, R. Chetrite, R. Chhaibi, J. Najnudel, and C. Pellegrini, Commun. Math. Phys. **387**, 1821 (2021).
[61] C. Liu, H. Tang, and H. Zhai, Phys. Rev. Res. **5**, 033085 (2023).
[62] S. R. Clark, J. Prior, M. J. Hartmann, D. Jaksch, and M. B. Plenio, New J. Phys. **12**, 025005 (2010).
[63] F. Minganti, A. Miranowicz, R. W. Chhajlany, I. I. Arkhipov, and F. Nori, Phys. Rev. A **101**, 062112 (2020).
[64] F. Minganti, A. Miranowicz, R. W. Chhajlany, and F. Nori, Phys. Rev. A **100**, 062131 (2019).
[65] S. Gupta, H. K. Yadalam, M. Kulkarni, and C. Aron, Phys. Rev. A **109**, L050201 (2024).
[66] M. A. Nielsen and I. L. Chuang, *Quantum Computation and Quantum Information* (Cambridge University Press, Cambridge, England, 2010), ISBN 9780511976667.
[67] J. P. Garrahan and I. Lesanovsky, Phys. Rev. Lett. **104**, 160601 (2010).
[68] J. L. Lebowitz and H. Spohn, J. Stat. Phys. **95**, 333 (1999).
[69] M. Esposito, U. Harbola, and S. Mukamel, Rev. Mod. Phys. **81**, 1665 (2009).
[70] F. Carollo, J. P. Garrahan, I. Lesanovsky, and C. Pérez-Espigares, Phys. Rev. A **98**, 010103(R) (2018).
[71] F. Carollo, J. P. Garrahan, and R. L. Jack, J. Stat. Phys. **184**, 13 (2021).
[72] M. Cech, I. Lesanovsky, and F. Carollo, Phys. Rev. Lett. **131**, 120401 (2023).
[73] W. H. Zurek, Rev. Mod. Phys. **75**, 715 (2003).
[74] M. Beau, J. Kiukas, I. L. Egusquiza, and A. del Campo, Phys. Rev. Lett. **119**, 130401 (2017).
[75] The stability and restrictions imposed by complete positivity will be studied in a follow-up article.
[76] C. M. Bender and S. Boettcher, Phys. Rev. Lett. **80**, 5243 (1998).
[77] W. Horsthemke and R. Lafever, *Noise-Induced Transitions*, Springer Series in Synergetics Vol. 15 (Springer, Berlin, Heidelberg, 2006).
[78] A. Uhlmann, Rep. Math. Phys. **9**, 273 (1976).
[79] D. Bures, Trans. Am. Math. Soc. **135**, 199 (1969).
[80] R. Jozsa, J. Mod. Opt. **41**, 2315 (1994).
[81] M. Hübner, Phys. Lett. A **163**, 239 (1992).
[82] F. Verstraete, M. M. Wolf, and J. Ignacio Cirac, Nat. Phys. **5**, 633 (2009).
[83] M. Motta, C. Sun, A. T. K. Tan, M. J. O'Rourke, E. Ye, A. J. Minnich, F. G. S. L. Brandão, and G. K.-L. Chan, Nat. Phys. **16**, 205 (2020).